Supplementary Materials for

An Inactivation Gate of the BsYetJ Calcium Channel That Becomes Functional in the Endoplasmic Reticulum Environment

Yu-Jing Lan[1], Chu-Chun Cheng[1], Shu-Chi Chu[1], Hung-Ying Chen[1], Chieh-Chin Li[1,2], Te-Yu Kao[1], and Yun-Wei Chiang[1]*

[1]Department of Chemistry, National Tsing Hua University, Hsinchu 300-044, Taiwan

[2]Department of Physiology and Biophysics, Weill Cornell Medical College, New York, NY 10065, USA

*Corresponding email: ywchiang@mx.nthu.edu.tw

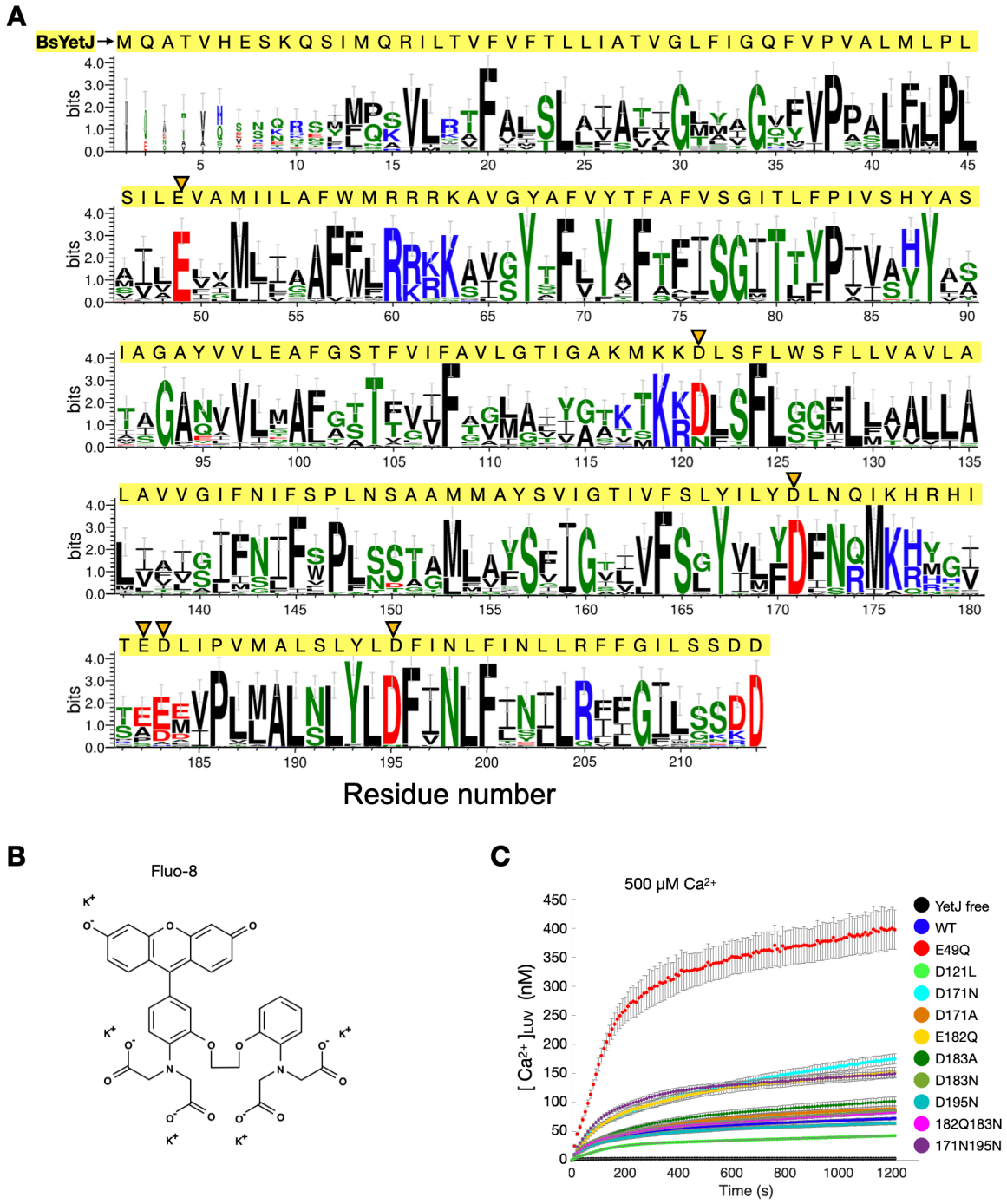

Figure S1. Information about the sequence analysis and the Fluo-8 molecule. (**A**) Sequence conservation of selected amino acids in BsYetJ. Totally 30 homologous sequences with more than 50% similarity are collected using HMMER search against UNIREF90 database by ConSurf web server (http://consurf.tau.ac.il/)[49,50]. Multiple Sequence Alignment was built using MAFFT and the conservation was depicted using WebLogo (http://weblogo.threeplusone.com/create.cgi)[51]. Conservation is measured in bits, each residue height shows the degree of conservation, and error bars represent sampling errors. Polar

amino acids are shown in green, hydrophobic amino acids are shown in black, positive and negative amino acids are shown in blue and red, respectively. The results indicate that these eight residues E49, D121, D171, E182, D183, D195, D213, D214 (denoted by yellow triangles) are highly conserved in BsYetJ and its homologs. Crystal results (PDB code: 4PGR, 4PGS) show D213 and D214, the last two residues in the BsYetJ sequence, are undetermined due to highly disordered. This study thus decided to investigate the first six residues among the highly conserved and considered them as the most important negatively charged residues. (**B**) Chemical structure of Fluo-8. (**C**) $[Ca^{2+}]_{LUV}$ data for 500 μM ∇Ca^{2+}.

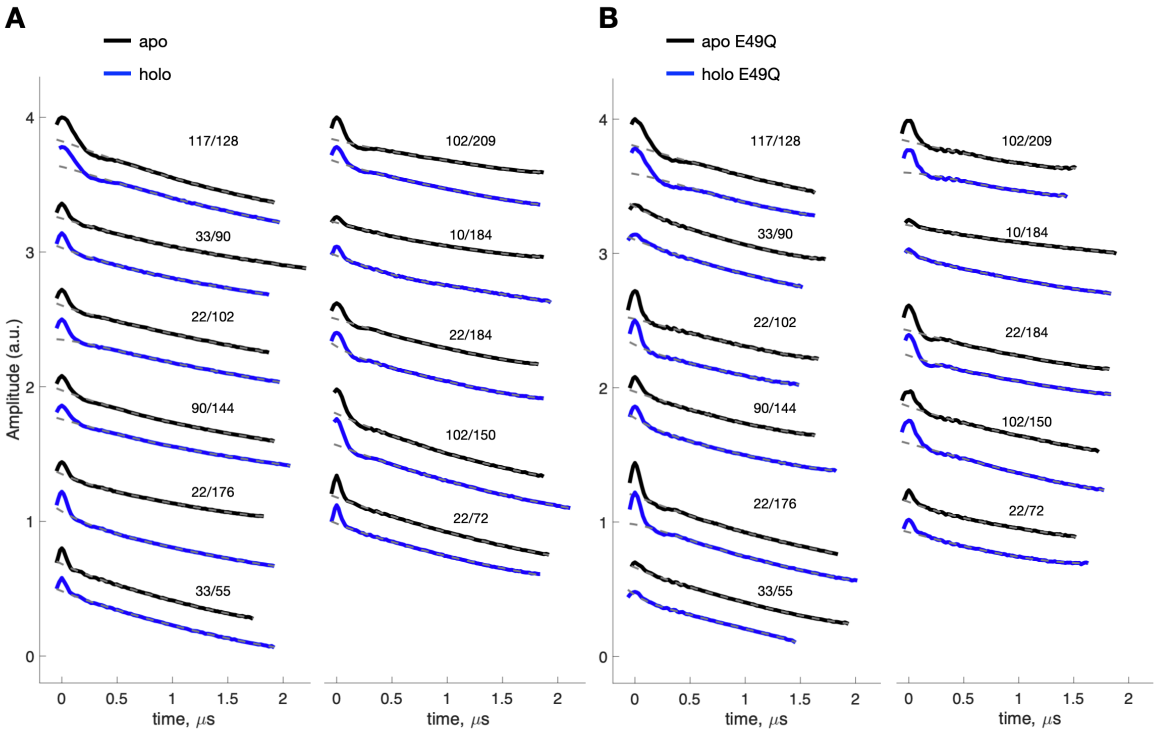

Figure S2. DEER measurements of spin-labeled BsYetJ in apo and holo states. (**A**) Primary DEER traces of the spin-labeled BsYetJ variants. (**B**) Primary DEER traces of the spin-labeled BsYetJ E49Q variants. (**C**) Uncertainty analysis of the DEER distance distributions of BsYetJ variants. The method to estimate the uncertainty (blue shaded area) in the distance distributions is given in Methods. (**D**) Uncertainty analysis of the DEER distance distributions of BsYetJ E49Q variants.

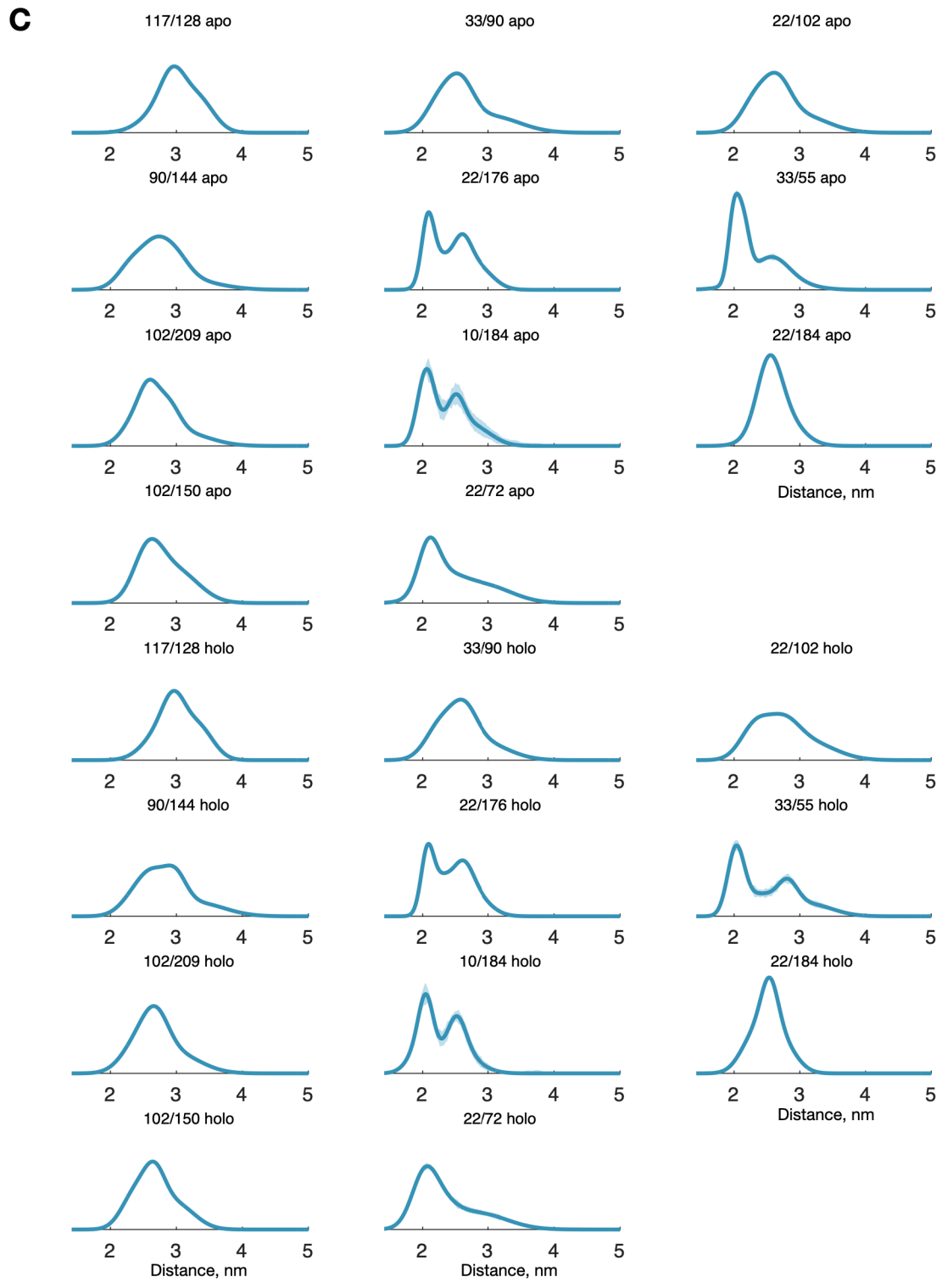

Figure S2. (continued)

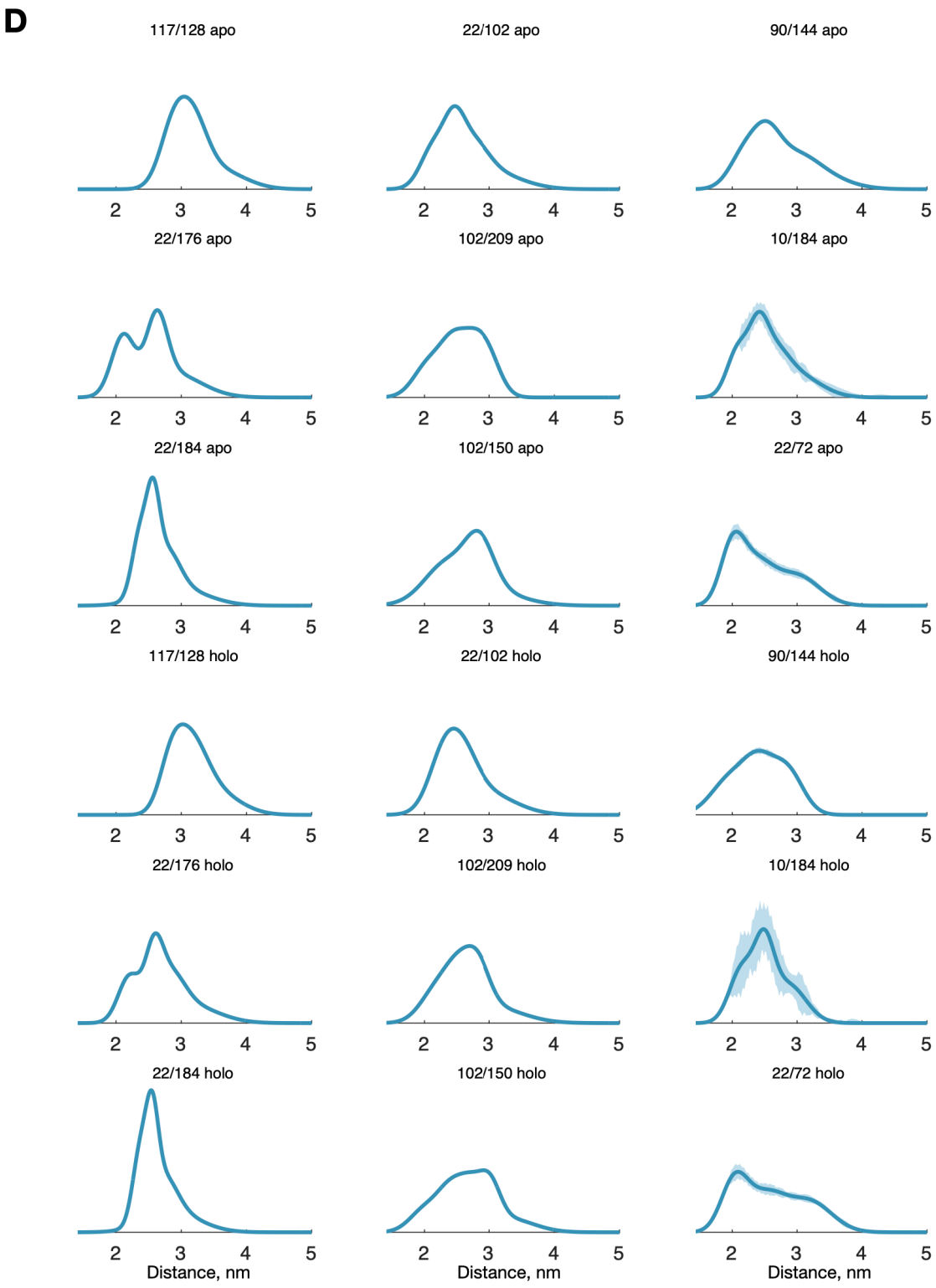

Figure S2. (continued)

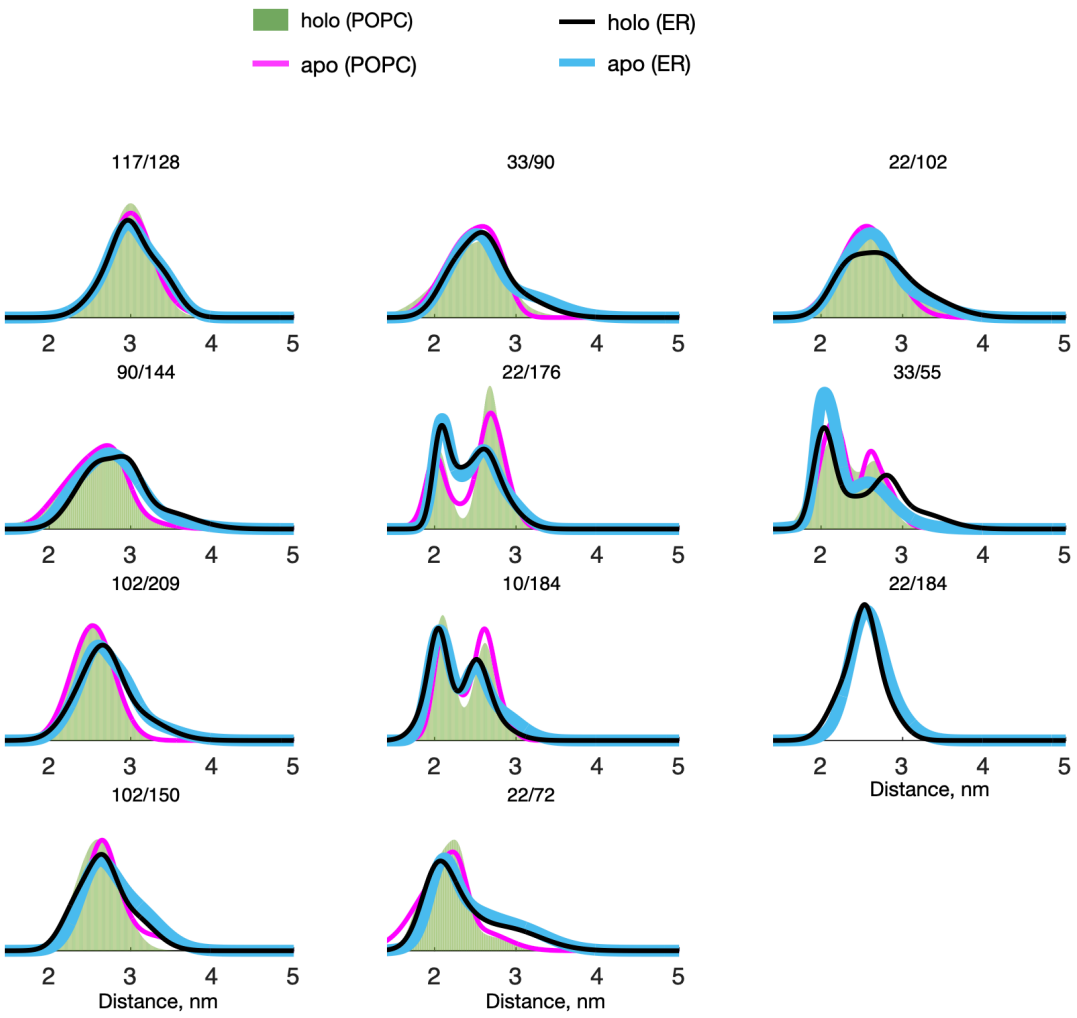

Figure S3. A comparison of the DEER results obtained in different lipid environments. A comparison of the distance distributions of spin-labeled BsYetJ, in apo and holo states, obtained in the pure POPC nanodiscs versus the ER lipid nanodiscs environments.

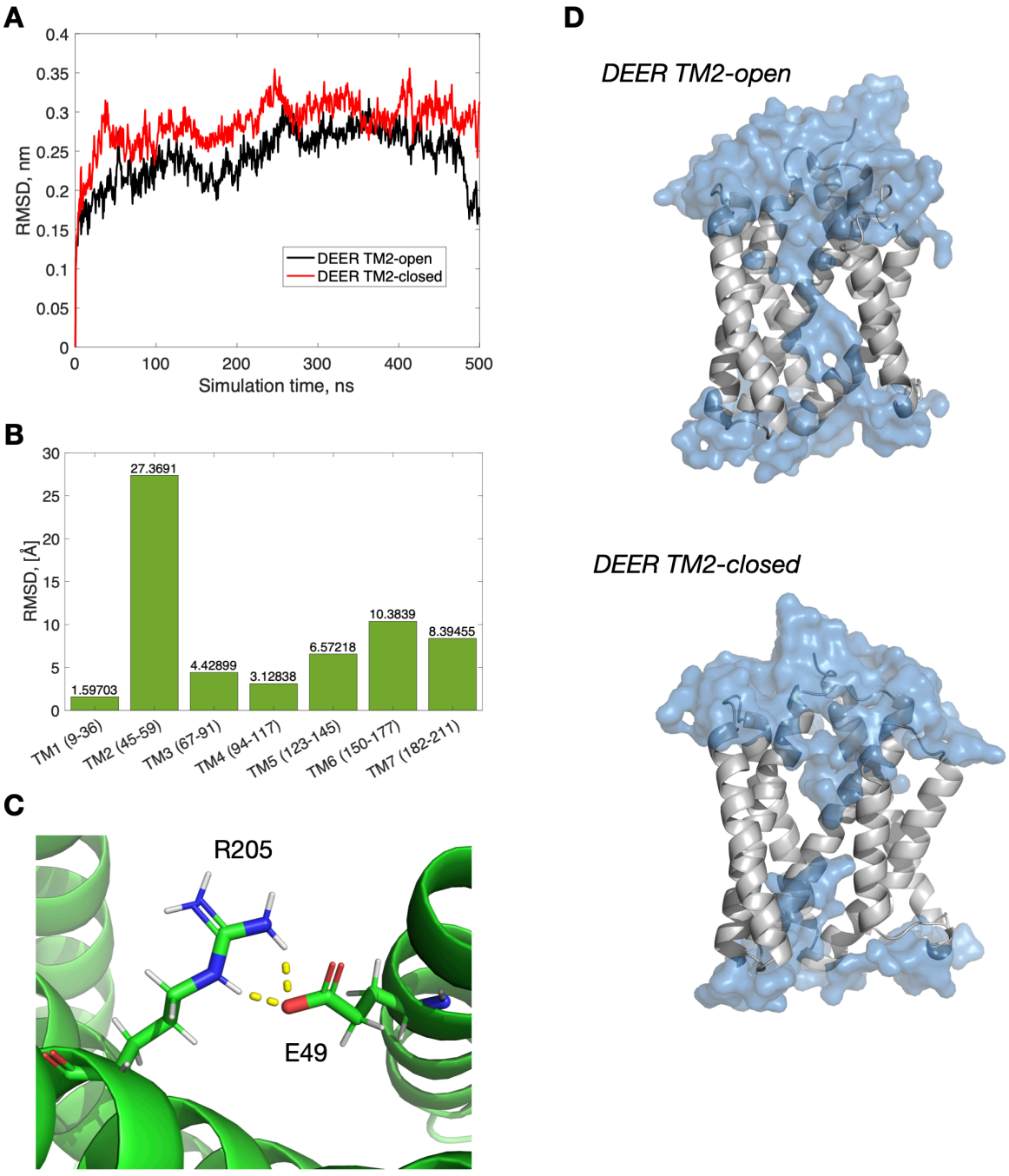

Figure S4. Results of the MD simulations and modeling. (**A**) RMSD values from the MD simulations to validate the two DEER-derived models, DEER TM2-open and -closed structures. RMSD is calculated from the root mean-square-average distances between Cα atoms of two superimposed structures (i.e., the initial and a MD-snapshot structure), providing a quantitative measure of how a modeled structure deviates from the initial structure during MD simulations. Overall, the RMSD values converged rapidly and became approximately constant for at least 400 ns. The converged values are in the range of 0.24 to

0.29 nm, indicating that the final and initial structures are similar. It supports that the initial structures derived from the DEER results are stable and reliable in the ER lipid environment. (**B**) RMSD values to quantitatively describe the differences of individual TM helices between the DEER TM2-open and -closed structures. (**C**) A MD snapshot of the DEER TM2-closed structure showing the hydrogen bonds between E49 and R205 observed in the MD simulations. A mean hydrogen bound number of 1.25 between E49 and R205 was found over the simulation time from 30 to 500 ns. (**D**) Results of the MD simulations showing water molecules can flow through the DEER TM2-open structure but are blocked in the DEER TM2-closed structure.

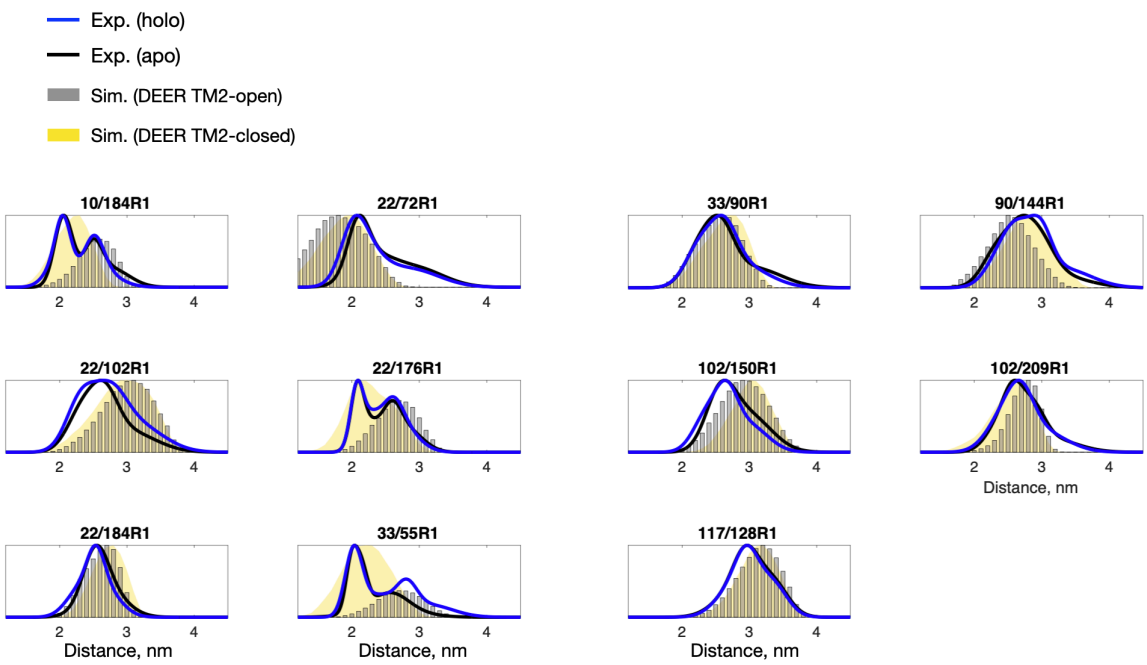

Figure S5. Distance distributions simulated from our DEER-derived models. Based on our DEER-derived models (Fig. 4A), we generated interspin distance distributions for the DEER TM2-open and -closed structures using the MtsslWizard program. The simulations (Sim.) are in a good agreement with the DEER experimental (Exp.) results in both apo and holo states.

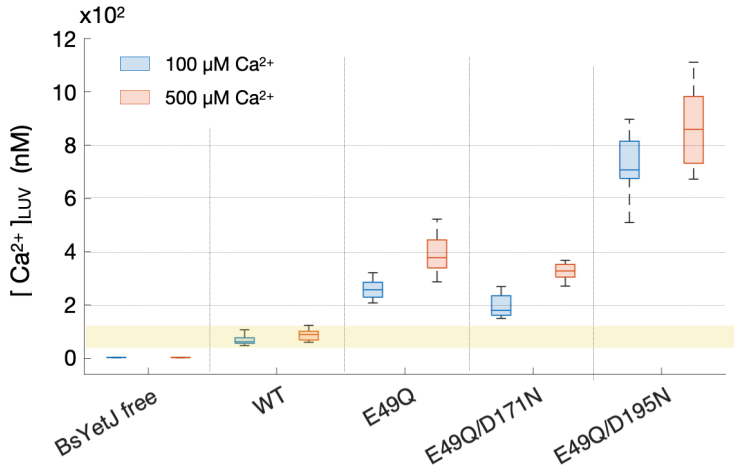

Figure S6. Calcium influx activity of E49Q/D171N and E49Q/D195N. To support our hypothesis that D171- or D195-associated sites act as a minor selectivity filter than E49 in controlling the calcium influx activity, we performed the calcium activity assay on two BsYetJ variants, E49Q/D171N and E49Q/D195N, each having two mutations at their two respective selectivity filters proposed in the present study. For a convenient comparison of the activity, we also provide the results of BsYetJ-free, WT, and E49Q. We found that $[Ca^{2+}]_{LUV}$ of E49Q/D171N is comparable to that of E49Q, but E49Q/D195N has a distinctly greater $[Ca^{2+}]_{LUV}$ than all other BsYetJ. As D195N alone is not sufficient to cause a large change in $[Ca^{2+}]_{LUV}$ (shown in Fig. 1E), our results here demonstrate that D195 acts as a relatively minor selectivity filter than E49 in determining the calcium influx activity and that D195 is more important than D171 in controlling the calcium influx activity of the minor selectivity filter.